A model of hoarfrost formation

Dr. Lasse Makkonen
VTT Technical Research Centre of Finland
Box 1000, 02044 VTT, Finland, *lasse.makkonen@vtt.fi*

***Abstract*—A time-dependent numerical model of hoarfrost formation on a cable is proposed. It is aimed at calculating the thickness of a hoarfrost layer using routinely measured meteorological data as input. The growth rate and density of hoarfrost are simulated. This requires continuous calculation of the surface temperature around the cable. Joule heating is included and considered as a possible means to prevent hoarfrost from forming. The model also simulates the disappearance of hoarfrost by evaporation, melting and dropping off. The feasibility of relating the corona loss on a high voltage overhead line with the modelled hoarfrost thickness is tested by field data.**

I. Introduction

HOARFROST forms when water vapour sublimates directly into solid ice. Under natural atmospheric conditions the resulting ice deposition consists of loosely spaced needle-like thin ice crystals (Figure 1). The dimensions of hoarfrost depositions are usually small and the density of them is very low. Hoarfrost is easily blown off by the wind. Consequently, hoarfrost alone does not cause ice loads or aerodynamic effects that are significant to structural safety, unlike rime, glaze and wet snow.

Nevertheless, hoarfrost causes problems, particularly on overhead cables. On power lines hoarfrost is known to be related to corona discharges [1]. The magnitude of corona losses in power transmission is at its greatest when the electric field at the conductor surface is enhanced by the presence of ice needles formed from hoarfrost deposition. The resulting corona losses are responsible for electricity transmission losses that are of significant economic value in cold regions. Furthermore, on overhead cables for trains hoarfrost causes a corona discharge at the contact with the pantograph, causing a light and noise problem.

Hoarfrost may also form in an intake channel of a turbine power plant. Under such conditions, the density of the accretions may be so high that they may cause damage to the turbine blades when released to the air flow.

During hoarfrost formation in nature the relative humidity of air is not necessarily high: The outgoing radiation may cool the surface so that sublimation occurs even at low humidity. When the relative humidity is close to or above 100% sublimation occurs even without the cooling effect. Thus, hoarfrost also forms combined with rime icing. The portion of the icing rate due to sublimation is then typically small. However, the rate of hoarfrost formation is approximately proportional to the surface area whereas the rate of rime icing increases much slower with increasing object size. Therefore, for ice load modelling on very large objects, hoarfrost needs to be taken into account. Also, very accurate modelling of rime icing for the rotating multi-cylinder method requires inclusion of sublimation [2].

Hence, there are several applications in which numerical modeling of hoarfrost formation is useful. The best prospect in utilizing hoarfrost modeling is in the significant savings to be achieved if hoarfrost formation on cables could be predicted using a high-resolution weather forecasting model or if it could be reduced by controlled Joule heating. Here a physical-numerical model of hoarfrost is proposed. In contrast to some other models for plates and for industrial applications [3 - 9], this model is developed specifically for simulating hoarfrost on cables in the natural outdoors environment.

Figure 1. Hoarfrost on a crabapple. Photo by Susanne von Schroeder.

II. THE MODEL

The foundation of this hoarfrost formation model is the horizontal cylinder icing model by Makkonen [10], discussed also in [11] and [12]. The additions made to that model for this study are:

1. A sub-program simulating sublimation rate and hoarfrost density is included, as explained below.
2. Free convection is taken into account in the heat balance because hoarfrost may form under no wind.
3. The heat balance and ice accretion are calculated separately on the windward side and the lee side, and on the upper side and lower side of the object.
4. Heat transfer from the conductor to the surface of ice is modeled. This allows including the effect of the Joule heating to the hoarfrost growth process.
5. The outgoing long wave radiation and Sun's direct radiation are included in the heat balance, since hoarfrost may form during clear skies.
6. Ice disappearance is modeled by including evaporation and melting, as well as a criterion of ice release when the surface temperature of the cable reaches 0°C. This makes long-term continuous modeling possible.
7. The model can be run when there is no rime icing or precipitation to simulate hoarfrost growth only. A necessary input then is the humidity of air.

A. Sublimation

The sublimation rate and evaporation rate are calculated by eq. (1).

$$I = \frac{0.62}{c_p p_a} \cdot h \cdot \left(e_s - e_a\right) \tag{1}$$

where c_p is the specific heat of air, p_a the atmospheric pressure, h the convective transfer coefficient and e_s and e_a the water vapor pressures over ice and in air, respectively. The convective transfer coefficient h depends essentially on wind speed and cable diameter. The equilibrium water vapor pressure over ice, e_s, depends on the surface temperature of the ice, the modeling of which is, therefore, a critical issue here. The vapor water pressure in air is an input parameter for the modeling.

B. Convective heat transfer

In the case of no wind, the convective heat transfer coefficient $h=k_a Nu/D$ is calculated separately on the upper side and lower side of the cable, and in the presence of wind separately on the windward and the leeward surfaces. Here k_a is the heat conductivity of air, D is the iced cylinder diameter and Nu is the Nusselt number.

The Nusselt number in free convection is calculated by [13]

$$Nu_v = 0.395\, Gr^{0.25} \tag{2}$$

where Gr is the Grashof number

$$Gr = \frac{gD^3\left|t_s - t_a\right|}{\upsilon^2\left(t_a + 273.15°C\right)} \tag{3}$$

Here g is the gravitational constant, υ is the cinematic viscosity of air, t_s the ice surface temperature and t_a the air temperature. Free convection calculated this way is assumed to affect the upper side of the cable when $t_s<t_a$ and the lower side of it when ts>ta.

For forced convection, i.e., at a wind speed v, the Nusselt number is calculated by the Reynolds number Re = vD/υ as

$$Nu_b = aRe^{\,0.85} \tag{4}$$

In eq. (4) the constant *a* is 0.032 for the windward side and 0.007 for the lee side. This equation gives allowance to the roughness of the ice surface [10].

The bigger of Nu_v and Nu_b is applied in the simulations.

C. Surface heat balance

Because hoarfrost forms also in clear skies, a detailed treatment of radiation in the heat balance is necessary. In fact, when there is no wind, the outgoing long wave radiation is the driving force for hoarfrost formation, as it cools the surface and thus lowers e_s.

The outgoing long wave radiation flux is calculated by eq. (5) which includes the assumption that the radiation fluxes from the ground and from the lower side of the cable cancel out. Here σ is the Stefan-Bolzmann coefficient.

$$q_{eff,0} = 0.5\sigma\left[\left(t_s + 273.15°C\right)^4 - \left(t_a + 273.15°C\right)^4\left(0.58 + 0.044\sqrt{e_a}\right)\right] \tag{5}$$

A correction for cloudiness is made by

$$q_{eff} = \left(1 - 0.08n\right)\, q_{eff,0} \tag{6}$$

where n is cloudiness in parts of ten.

Short wave radiation by the Sun may also be included as a separate input to the modeling. It is usually a small term, however, because the formation of hoarfrost typically occurs during night time and because the ice surface has a very high optical reflection coefficient.

The thermal inertia of the cable is taken into account in the time-dependent simulations. The Joule heating q_i is used as an input in the calculation of the temperature t_s of the ice surface but also of t_w, the temperature at the ice/cable interface. The latter is calculated by

$$t_w = t_s + q_i l / k_i \tag{7}$$

where *l* is the thickness of the simulated hoarfrost deposit and k_i is its mean heat conductivity. The heat conductivity k_i in W/(mK) is estimated by

$$k_i = 0.0242 + 0.2\rho_{TOT} + 2.54\rho_{TOT}^2 \tag{8}$$

where ρ_{TOT} is the simulated overall hoarfrost density in g/cm^3.

Equation (8) is a modified extension of an empirical equation given in [14].

When the model shows no ice, the surface temperature is calculated without the sublimation/evaporation term.

D. Hoarfrost density

The density of the forming hoarfrost ρ (in g/cm^3) is calculated based on the mean surface temperature of the windward side of the cylinder by eq. (9) presented in [4] based on experimental data in the range -25 °C < t_s < 0 °C and 2 m/s < v < 6 m/s.

$$\rho = 0.65\, e^{0.227\, t_s} \qquad (9)$$

The density of the overall accretion ρ_{TOT} and the thickness of the ice layer are calculated cumulatively after each time-step as in [10]. When there is disappearance of ice, its density is assumed to be that of the overall density.

III. Running the Model

The model is programmed in Visual Basic. The input can be given manually or be read directly e.g. from synoptic meteorological observation data. In the latter case the output is given at intervals of three hours. However, the internal calculation time-step is much shorter for better accuracy. It is 9 seconds for the first 10 minutes of icing and 360 seconds after that.

The simulation for a power line cable requires as input

- Cable diameter
- Cable specific heat capacity
- Joule heating by the cable
- Wind speed
- Air temperature
- Relative humidity in air
- Cloudiness

The model also requires a non-zero value for the liquid water content and the median volume droplet diameter if rime icing occurs simultaneously. During clear skies Sun's radiation may be given as input, too.

IV. Results and Discussion

Test runs using data of four Finnish synoptic weather stations in January-April 1994 showed that the model predicts a hoarfrost thickness of 0 - 13 mm, which corresponds to observations in nature. The results showed systematic variations according to the time of day, as one would expect (Figure 2). Hoarfrost typically forms in the night and disappears during the day according to the simulation results.

The hoarfrost modeling results based on the synoptic weather were compared with data for the corona loss on a 360 km long 400kV overhead power line as measured by a power utility IVO Voimansiirto Oy. The results showed a significant correlation between the predicted occurrence of hoarfrost and the measured corona loss, particularly when the events with precipitation occurrence were removed from the data.

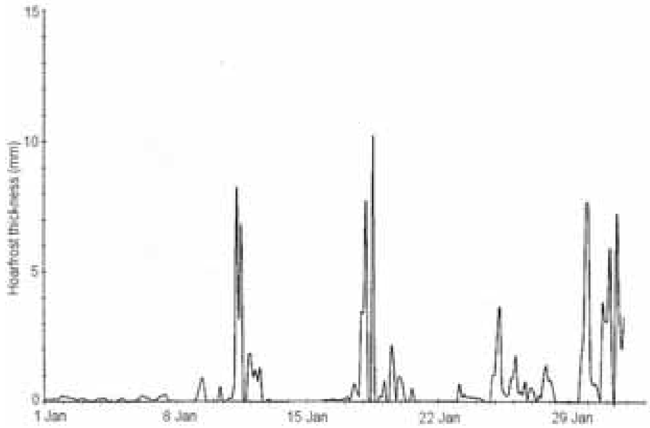

Figure 2. An example of model output for a power line cable when using synoptic weather data (Kajaani, Finland, 1994).

The hoarfrost modeling results based on the synoptic weather were compared with data for the corona loss on a 360 km long 400kV overhead power line as measured by a power utility IVO Voimansiirto Oy. The results showed a significant correlation between the predicted occurrence of hoarfrost and the measured corona loss, particularly when the events with precipitation occurrence were removed from the data.

There was only a very weak correlation between the thickness of the hoarfrost accretion and the measured quantitative corona loss, however. This may be due to weaknesses in the modeling e.g. in that the electric field on the cable may affect the hoarfrost formation [15]. It is unlikely that this result would be related to feedback between the corona discharge and ice structure and amount, because such interactions are weak [16]. Overall, it appears that the above mentioned low correlation is mostly due to the following problem in the input data.

The model results critically depend on the input for the humidity in air. As long as the surface temperature is not significantly lower than the air temperature, sublimation occurs in air that is supersaturated with respect to ice. The degree of super-saturation then controls the growth rate of hoarfrost. The supersaturation, however, is not indicated at all by the routine weather station data because of icing (formation of hoarfrost!) of the humidity probes [17]. The conventional humidity probes show a value locked at the saturation when the correct value is above it [17]. This removes from the data the real variation in the air humidity in supersaturated conditions, and thus largely prevents detecting the correlation between the modeled and real hoarfrost thickness. The model should be tested with data based on humidity measurements by a heated probe.

Test runs were also made to find out the sensitivity of hoarfrost formation to various parameters. The results are quite sensitive to cloudiness, for example. Of particular interest here is that these simulations showed a significant reduction in the frequency of hoarfrost by a rather small increase in the Joule heating. This may provide means to control the hoarfrost formation on power lines in order to reduce corona losses.

V. Acknowledgment

This work was originally supported by IVO Voimansiirto Oy, which also provided transmission loss data for model comparisons.

VI. References

[1] K. Lahti, M. Lahtinen and K. Nousiainen, ”Transmission line corona losses under hoar frost conditions”, *IEEE Trans. Power Delivery*, vol. 12, pp. 928-933. 1997.

[2] L. Makkonen, ”Analysis of rotating multicylinder data in measuring cloud-droplet size and liquid water content”, *J. Atmos. Oceanic Technology*, vol. 9, pp. 258-263. 1992.

[3] H.W. Schneider, ”Equation of the growth rate of frost forming on cooled surfaces”, *Int. J. Heat Mass Transfer*, vol. 21, pp. 1019-1024. 1977.

[4] Y. Hayashi, A. Aoki and H. Yuhara, ”Study of frost formation based on a theoretical model of the frost layer”, *Heat Transfer-Japanese Res.*, vol. 6, pp. 79-94, 1977.

[5] H. Saito, I. Tokura, K. Kishinami and S. Uemura, ”A study on frost formation”, *Trans. Japan Soc. Mech. Engr.,* Ser B, vol. 50, pp. 1190-1195. 1984. (in Japanese).

[6] N. Seki, S. Fukusako, K. Matsuo and S. Uemura, ”Incipient phenomena of frost formation”, *Trans. Japan. Soc. Mech. Engr*., Ser B, vol. 50, pp. 825-831. 1984. (in Japanese).

[7] R. Östin and S. Andersson, ”Frost growth parameters in a forced air stream”, *Int. J. Heat Mass Transfer*, vol. 34, pp. 1009-1017. 1991.

[8] S.P. Raju and S.A. Sherif, ”Frost formation and heat transfer on circular cylinders in cross flow”, *Fundamentals of Heat Transfer in Porous Media*, vol. 193. ASME, pp. 109-121. 1992.

[9] P.J. Mago and S.A. Sherif, “Frost formation and heat transfer on a cold surface in ice fog”, *Int. J. Refrigeration*, vol. 28, pp. 538-546. 2005.

[10] L. Makkonen, ”A model of ice accretion on wires”, *J. Climate Applied Meteorol.*, vol. 23, pp. 929-939. 1984.

[11] L. Makkonen, ”Models for the growth of rime, glaze icicles and wet snow on structures”, *Phil. Trans. R. Soc. Lond.* A, vol. 358, pp. 2913-2939. 2000.

[12] G. Poots, ”*Ice and Snow Accretion on Structures*”, Wiley & Sons, 1996, pp. 80-83.

[13] H. Sparrow and A.J. Stretton, ”Natural convection from variously oriented cubes and from other bodies of unity aspect ratio”, *Int. J. Heat Mass Transfer*, vol. 28, pp. 741-752. 1985.

[14] J.D. Yonko and C.F. Sepsy, ”An investigation of the thermal conductivity of frost while forming on a flat horizontal plate”, *ASHRAE Trans*., vol. 73, Part II, Paper no. 2043, pp. I1.1-I1.10. 1967.

[15] Y. Teisseyre and M. Farzaneh, ”On the mechanisms of the ice accretion on H.V. conductors”, *Cold Regions Sci. Technol.*, vol. 18, pp.1-8. 1990.

[16] X.H. Zhang, Z.L. Liu, J.T. Wang, Y.J. Gou, S. Meng and C.F. Ma, ”Experimental investigation of the influence of electric field on frost layer growth under natural convection condition”, *Prog. Natural Sci.*, vol. 16, pp. 410-415. 2006.

[17] L. Makkonen and T. Laakso, ”Humidity measurements in cold and humid environments”, *Boundary-Layer Meteorol.*, vol. 116, pp. 131-147. 2005.